Geochemistry Geophysics Geosystems G3
AN ELECTRONIC JOURNAL OF THE EARTH SCIENCES
Published by AGU and the Geochemical Society

Article
Volume 9, Number 12
16 December 2008
Q12018, doi:10.1029/2008GC002127
ISSN: 1525-2027

Tracking provenance change during the late Miocene in the eastern Mediterranean using geochemical and environmental magnetic parameters

C. M. Köhler
FB Geowissenschaften, University of Bremen, Postfach 330440, D-28334 Bremen, Germany (ckoehler@uni-bremen.de)

Paleomagnetic Laboratory "Fort Hoofddijk," University of Utrecht, Budapestlaan 17, N-L3584 CD Utrecht, Netherlands

D. Heslop
FB Geowissenschaften, University of Bremen, Postfach 330440, D-28334 Bremen, Germany

M. J. Dekkers, W. Krijgsman, and D. J. J. van Hinsbergen
Paleomagnetic Laboratory "Fort Hoofddijk," University of Utrecht, Budapestlaan 17, N-L3584 CD Utrecht, Netherlands

T. von Dobeneck
FB Geowissenschaften, University of Bremen, Postfach 330440, D-28334 Bremen, Germany

[1] Marls of the Metochia section (Gavdos, Greece) have been analyzed using geochemistry, environmental magnetism, and diffuse reflectance spectrometry to study late Miocene paleoenvironmental changes in the eastern Mediterranean region. Fuzzy *c*-means cluster analysis (FCM), combined with nonlinear mapping (NLM), has been performed on a multiparameter data set to identify and characterize terrigenous source areas from North Africa and the Aegean margin. The parameters included in the FCM were selected on the basis of their univariate characteristics and their ability to trace input changes from regional source areas. The hard isothermal remanent magnetization (HIRM), calculated on a carbonate-free basis, and the Ti/Al ratio are used to distinguish aeolian dust and transport mechanisms of material originating from North Africa. Mass accumulation rates of Al and Ni are employed to represent the input of terrigenous material originating from the Aegean region. $CaCO_3$, calculated from Ca abundance, provides information concerning marine productivity and Mn/Al is used to trace reductive diagenesis in the marls. After performing the FCM and NLM analysis, a four-cluster solution has the greatest stability and describes paleoenvironmental changes in both the African and European source areas. The cluster solution clearly reveals the change from input dominated by terrigenous material in the lower parts of the Metochia section to marine input at the top of the section but also reveals changes in paleoenvironmental conditions in North Africa from arid to more humid conditions at ~8.2 Ma.

Components: 7970 words, 6 figures, 2 tables.

Keywords: geochemical parameters; rock magnetism; fuzzy *c*-means cluster analysis; paleoenvironment; eastern Mediterranean.

Index Terms: 1616 Global Change: Climate variability (1635, 3305, 3309, 4215, 4513); 1512 Geomagnetism and Paleomagnetism: Environmental magnetism; 1050 Geochemistry: Marine geochemistry (4835, 4845, 4850).

Received 14 June 2008; **Revised** 29 September 2008; **Accepted** 8 October 2008; **Published** 16 December 2008.

Köhler, C. M., D. Heslop, M. J. Dekkers, W. Krijgsman, D. J. J. van Hinsbergen, and T. von Dobeneck (2008), Tracking provenance change during the late Miocene in the eastern Mediterranean using geochemical and environmental magnetic parameters, *Geochem. Geophys. Geosyst.*, *9*, Q12018, doi:10.1029/2008GC002127.

1. Introduction

[2] The relationships between different parameters, especially when combining geochemistry and environmental magnetism, are often complex. However, subtle, but important, changes can be identified and better interpreted when applying fuzzy *c*-means cluster analysis (FCM) [*Bezdek*, 1981], which is commonly combined with the nonlinear mapping (NLM) dimension reduction technique [*Sammon*, 1969]. When both techniques indicate similar groupings, the cluster solution becomes more interpretable [*Vriend et al.*, 1988; *Dekkers et al.*, 1994]. FCM is a powerful tool to unravel changes in paleoenvironmental information recorded in sediments [*Dekkers et al.*, 1994; *Kruiver et al.*, 1999; *Schmidt et al.*, 1999; *Urbat et al.*, 2000; *Hanesch et al.*, 2001; *Kruiver et al.*, 2002; *Vlag et al.*, 2004]. It is important to have well-defined input variables, with precise interpretations assigned to them, in order to be able to understand and interpret the clustering solution. The aim of this study was to investigate uplifted marine marls from the Metochia section on Gavdos Island (located South of Crete [*Krijgsman et al.*, 1995]), using FCM applied to a carefully chosen geochemical and environmental magnetic data set, to discriminate between the different European and African input sources and to identify changes in sediment provenance.

[3] The astronomically dated marl-sapropel sequences of the Metochia B and C sections provide an environmental archive spanning the time interval from 9.4 to 6.9 Ma, from which sediment supply and environmental conditions in source areas such as the former southern Aegean landmass and northern Africa can be reconstructed (Figure 1). Sulfate-reducing diagenesis in sapropel layers can modify strongly the primary terrigenous input signal [e.g., *Passier et al.*, 1998]; therefore only samples from the marls were selected for analysis.

[4] Different approaches have been adopted to identify the sediment sources to the eastern Mediterranean Sea. For example, *Venkatarathnam and Ryan* [1971] used seafloor sediments and *Foucault and Mélières* [2000] associated clay mineral assemblages with European and African sources. North African dust can be traced by identifying hematite and goethite, which provide information concerning the abundance of transported dust [*Larrasoaña et al.*, 2003a]. Geochemical data in the eastern Mediterranean region can enable discrimination between materials originating from the Aegean or North Africa [*Bergametti et al.*, 1989; *Wehausen and Brumsack*, 1998; 2000; *Lourens et al.*, 2001].

[5] Previous investigations demonstrated that Al and Ca, and the ratios Ni/Al, Si/Al, Fe/Al, and Ti/Al are indicative of different sediment origins and can be linked to environmental conditions in certain source areas [e.g., *Bergametti et al.*, 1989; *Wehausen and Brumsack*, 1998; *Lourens et al.*, 2001]. Ni is associated with ultramafic rocks, which in this area are exclusively found in the Aegean region, whereas Si/Al and Ti/Al represent the African sources [*Wehausen and Brumsack*, 2000]. On the basis of these classifications, *Lourens et al.* [2001] and *Larrasoaña et al.* [2003a] employed specific elemental ratios to reconstruct changes in the Pliocene-Pleistocene climate of North Africa. The geochemistry of Miocene sediments is of interest because data can be compared to those from the Pliocene records of *Wehausen and Brumsack* [1998, 2000], who worked on Ocean Drilling Program (ODP) Site 969 (south of Crete), which contains a mixture of sediments from Aegean and North African sources. By using the precise astronomical age model of the Metochia sediments and by selecting a meaningful environmental data set, we will show that FCM can identify changes in sedimentary provenance and paleoenvironmental conditions in the source areas.

2. Metochia Section and Sampling

[6] Gavdos is situated 30 km to the South of Crete and represents the southernmost exposed part of the Hellenic arc. The Metochia section is in northeastern Gavdos and is composed of tectonically uplifted open marine sediments (Figure 1). The

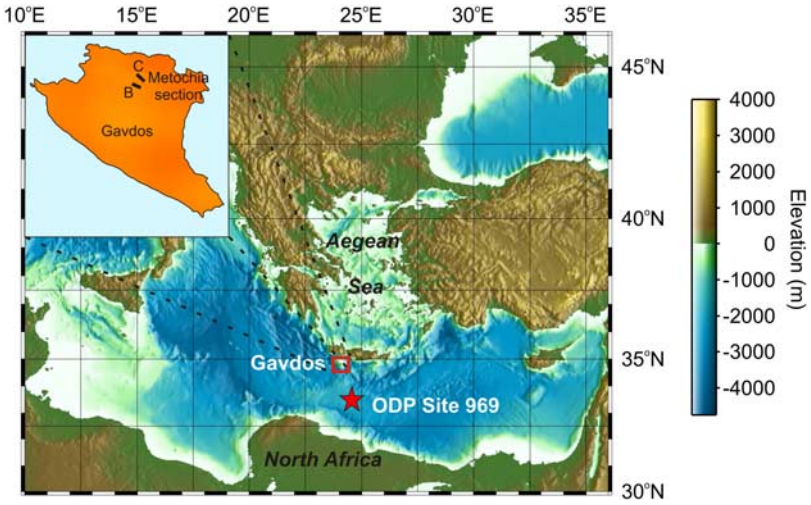

Figure 1. Map of the eastern Mediterranean region with the location of the Metochia section on Gavdos (South of Crete) between the Aegean rim and North Africa and the location of Ocean Drilling Program Site 969. (Inset shows Gavdos and the location of the Metochia section.)

sedimentation history of the Gavdos basin and the position of the Metochia section on the Aegean rim make it an ideal location for recording regional paleoenvironmental events. Paleobathymetry of the Metochia section, based on the contribution of planktonic species to the total foraminifera assemblage, indicates that Gavdos was situated at a water depth of more than 1000–1200 m during the late Miocene [*van Hinsbergen and Meulenkamp*, 2006].

[7] The section is composed of two subsections, Metochia B and C, with characteristic intercalated hemipelagic marls and sapropels [*Krijgsman et al.*, 1995]. The base of Metochia B consists of shallow marine sands [*Postma et al.*, 1993; *Krijgsman et al.*, 1995], which were not considered for this study because they mainly consist of locally derived clastic sediments. The Metochia sediments were precisely dated using combined cyclostratigraphic, magnetostratigraphic, and biostratigraphic methods [*Hilgen et al.*, 1995; *Krijgsman et al.*, 1995]. *Krijgsman et al.* [1995] identified 17 magnetic polarity reversals within the Metochia section that could be correlated to the geomagnetic polarity timescale (GPTS) [*Cande and Kent*, 1995] and that spanned the age interval from 9.6 to 6.9 Ma.

[8] The Metochia sapropel pattern was originally tuned by *Hilgen et al.* [1995] to the 65°N summer insolation curve of *Laskar* [1990], with modern-day values for dynamical ellipticity of the earth and tidal dissipation by the moon. Individual sapropels were correlated to precession minima, while small- and large-scale sapropel clusters were matched to maxima in the 100 and 400 ka eccentricity cycles, respectively [*Hilgen et al.*, 1995]. The coherent cyclicity of the Metochia sediments resulted in the section becoming a fundamental component of the stratigraphic framework for the Mediterranean Upper Miocene and played a key role in the extension of the astronomical polarity timescale from ~5 to 10 Ma [*Hilgen et al.*, 1995]. Revised sapropel ages in accordance with the more recent orbital solution of *Laskar et al.* [2004] are used here. These updates to the age model are in the range of 0.15–15.2 ka, which results on average in a 2.5 ka shift to younger ages.

[9] Samples collected by *Krijgsman et al.* [1995] were used here. In general, two to four fresh samples were selected from each marl bed (average spacing of 20 cm), with the number of samples depending on the thickness of each bed and the availability of material. 208 samples were investigated; however, no samples were available for three marl intervals (Metochia B: 8.839–8.821 Ma, Metochia C: 7.826–7.817 Ma, and 7.798–7.786 Ma).

3. Methods

[10] In order to reconstruct a sedimentary history from the Metochia section, it is necessary to use parameters that enable discrimination between the terrigenous contributions originating from the various source areas around the eastern Mediterranean. Suitable geochemical ratios are combined with environmental magnetic parameters and diffuse

reflectance data to characterize the Metochia sediments. The information provided by the various measured parameters is too complex to be unraveled by univariate or bivariate approaches; therefore FCM and NLM methods will be employed to determine how the different parameters are environmentally associated and controlled.

3.1. Geochemistry

[11] Terrigenous Al is a constituent of clays and silts, which are transported to the eastern Mediterranean from the Aegean region and North Africa via both aeolian and fluvial pathways [*Foucault and Mélières*, 2000; *Lourens et al.*, 2001]. Al abundance is important in geochemical interpretations because the abundances of other elements can be normalized against it to compensate for dilution effects [*Wehausen and Brumsack*, 1998]. $CaCO_3$ was calculated from Ca, assuming that 98% of the Ca resides within $CaCO_3$, which provides a proxy representing marine biogenic input. In contrast to the sapropel layers that form under humid conditions, with high fluvial runoff and low $CaCO_3$ content [*Schenau et al.*, 1999], eastern Mediterranean marls are rich in $CaCO_3$. Pleistocene marls from this region, for example, contain between ~52 and ~62% $CaCO_3$ [*Wehausen and Brumsack*, 1998]. More arid conditions during periods of marl formation result in reduced fluvial runoff and increased transport of northern African aeolian material to the eastern Mediterranean.

[12] Dust originating from North Africa is rich in both Si and Fe; hence Si/Al and Fe/Al have been used to identify and trace North African aeolian dust [*Bergametti et al.*, 1989; *Chiapello et al.*, 1997]. Fluctuations in Ti/Al reflect variations in the relative importance of fluvial and aeolian transport mechanisms because Ti is associated with aeolian dust, whereas Al is found in both aeolian and smectite-rich fluvial materials from both Aegean and North African sources [*Lourens et al.*, 2001]. When both Ti and Al have a North African origin, higher values of Ti/Al indicate a predominantly aeolian flux, while lower ratios signify fluvial transport [*Lourens et al.*, 2001; *Larrasoaña et al.*, 2003a].

[13] The characteristic Jurassic and Cretaceous ultramafic rocks found in Aegean mountains [*Jacobshagen*, 1986], including modern day Crete, provide a signature that can be distinguished from North African terrigenous material. Ni and Mg are associated with these rocks [*Wedepohl*, 1969; *Wehausen and Brumsack*, 2000]. Ni is only associated with Aegean sources, whereas Mg can also be present in clays derived from North Africa, e.g., palygorskite, thus the Mg content is ambiguous. Ni, instead of Mg, is therefore used to trace Aegean sources.

[14] To test for the possible influence of diagenetic processes on the marl samples and the presence of unidentified oxidized sapropels in the section [*Larrasoaña et al.*, 2006], the Mn/Al ratio is compared to the Fe/Al ratio for coincidence of peaks. Both Mn and Fe are mobilized and reprecipitated by downward diffusing oxidation during early diagenesis [*van Santvoort et al.*, 1997; *Kouwenhoven et al.*, 1999; *Kouwenhoven et al.*, 2003]. Detection of oxidized sapropels is important because Ni is enriched in sapropels [*van Santvoort et al.*, 1997; *Wehausen and Brumsack*, 2000] and diagenetic enrichment must be distinguished from a detrital Aegean signal.

[15] To determine the geochemical composition of the Metochia marls, X-ray fluorescence (XRF) analysis was performed on the planar surfaces of solid cylindrical samples (~4 g) using a *Spectro Xepos* energy dispersive polarization X–ray fluorescence analyzer. The measuring time was 300 s per sample. Accuracy and precision were checked using the internal marine standard Mag-1 (certified USGS marine sediment standard reference material) and duplicate measurements. Measurement errors are <5% for the elements employed here. For Al and Ni, mass accumulation rates (MAR) were calculated by taking the product of the XRF results (mg/kg), bulk density (kg/m^3), and sedimentation rate (m/ka) [*Peterson et al.*, 2000].

3.2. Environmental Magnetism

[16] To complement the geochemical data set, several magnetic parameters were measured. Magnetic susceptibility and the "hard" isothermal remanent magnetization (HIRM) are important tracers of terrigenous material. The volume-dependent magnetic susceptibility (κ), when calculated on a carbonate-free basis (cfb), provides a measure of the total magnetic mineral concentration, which in the case of marine sediments will be predominantly linked to the terrigenous magnetite content [*deMenocal et al.*, 1991]. Paramagnetic clay minerals can also contribute to κ. Their contribution becomes important when the concentration of magnetite is low. The value of κ was measured

on individual samples using a *KLY2 AGICO Kappabridge* instrument (noise level $\sim 4 \times 10^{-8}$ SI).

[17] Hematite and goethite are important constituents of North African dust [e.g., *Bloemendal et al.*, 1992]. Their high coercivity means that they are magnetically "harder" than ferrimagnetic materials such as magnetite. The carbonate free HIRM ($HIRM_{cfb}$) provides a measure of the antiferromagnetic mineral component. Each sample was pulsed in a 2.5 T field in order to at least partially magnetize the hematite and goethite component, yielding the isothermal remanent magnetization ($IRM_{2.5T}$), which was subsequently demagnetized with a backfield of −0.3 T to allow calculation of HIRM [*King and Channell*, 1991; *Stoner et al.*, 1996]. After each treatment in the pulse magnetizer, individual samples were measured on a 2-G *Enterprises DC*-SQUID magnetometer (noise level $\leq 1 \times 10^{-12}$ Am^2). HIRM was used to assess the combined abundance of the hematite and goethite components.

3.3. Diffuse Reflectance Spectrometry

[18] In addition to their magnetic properties, hematite and goethite are strong pigmenting minerals. Even in trace amounts they can exert a significant influence on the reflectance characteristics of a sediment [*Deaton and Balsam*, 1991]. Diffuse reflectance spectrometry (DRS) measures the ratio of incident to reflected light intensity as a function of wavelength. DRS spectra spanning the wavelengths of visible light (400–700 nm, in 10 nm increments) were determined for all samples using a Minolta CM-2002 spectrophotometer. The dominant wavelength of a measured spectrum (which is linked to the hue of the sediment color) can provide important information concerning hematite and goethite content [*Cornell and Schwertmann*, 1996]. Specifically, the dominant wavelength of mixtures of hematite and goethite are in the range of 580–595 nm [*Madeira et al.*, 1997]. The dominant wavelength of each Metochia sample was determined from the measured reflectance spectra to identify possible compositional changes within the terrigenous component.

3.4. Fuzzy *c*-Means Clustering and Nonlinear Mapping

[19] The aim of FCM is to define the similarities and dissimilarities that exist between a collection of points within a multivariate data space. A given number of so-called cluster centers are represented as points within the data space and the similarity of each measured sample can be compared to the individual cluster centers based upon a predefined distance metric. Memberships define the similarity of the points to the cluster centers, with values varying between zero (no similarity) and one (identical) for each cluster center, under the constraint that for any given sample the memberships across all the cluster centers must sum to unity. Identification of the optimal cluster centers is an iterative procedure based upon an objective function that aims to find a balance between producing the maximum separation between cluster centers and minimizing the combined distance between the samples and the cluster centers. It is possible that a given sample may not have a strong similarity with any of the given cluster centers. In this study, any sample for which $u_2 > 0.75u_1$ (with u_1 indicating the highest membership and u_2 the second highest membership) was assigned as a "transitional" case. The fuzzy exponent, q, which determines the fuzziness of the model, was chosen to be $q = 1.5$ [*Bezdek et al.*, 1984]. Before performing the FCM, the distribution of each parameter was normalized with a mean of zero and standard deviation of one to ensure that all parameters have equal weight. A number of FCM solutions were calculated with between two and nine cluster centers using the software of *Vriend et al.* [1988]. The stability of the cluster solution was tested by repeating the analysis from different starting configurations but also by including and excluding different input parameters. The final solution is therefore considered to be robust.

[20] NLM is a dimension reduction technique, which attempts to form an undistorted low-dimensional (typically two-dimensional) representation of a multidimensional data set [*Sammon*, 1969]. This is achieved by iteratively searching for a configuration of points in a low-dimensional space that accurately preserves the distance matrix that describes the relative positions of the data points in the high-dimensional measurement space. When FCM and NLM have similar sample groupings, it supports and adds meaningfulness to the cluster solution [*Vriend et al.*, 1988; *Dekkers et al.*, 1994]. NLM has therefore been used in combination with FCM to confirm a given cluster solution.

[21] Input parameters for the FCM and NLM were carefully chosen under the criterion that in order to be included in the analysis, a parameter must have a clear interpretation and must not represent the same process as another parameter. The input

parameters were therefore not biased due to over-representation of any given process.

4. Results and Interpretation

4.1. Univariate Statistics

[22] Source identification and variation of terrigenous input from different eastern Mediterranean sources is discussed based on the measured geochemical and magnetic parameters. Given that the marl-sapropel formation mechanism has not changed from the late Miocene through to the Pleistocene [*Schenau et al.*, 1999], the results of this study are compared to data from Pliocene sediments from ODP Site 969 (Figure 1). Owing to different land-water distributions in the Aegean region resulting from tectonic reorganizations during the late Miocene [*Meulenkamp and Hilgen*, 1986; *Meulenkamp et al.*, 1994; *van Hinsbergen and Meulenkamp*, 2006], comparisons may not be straightforward. However, both ODP Site 969 and the Metochia section should contain mixed Aegean and North African terrigenous components.

[23] Ti/Al for the Metochia marls are on average 0.057 (Figure 2), which is lower than for Pleistocene marls from ODP Site 969, which range from ~0.07 to 0.08 (sapropel values are ~0.06) [*Wehausen and Brumsack*, 2000]. Higher Ti/Al ratios observed in Site 969 marls are associated with Ti-rich North Africa aeolian dust [*Lourens et al.*, 2001; *Larrasoaña et al.*, 2003a]. The observation that marls of the Metochia section have Ti/Al ratios in the same range as Pliocene sapropels could result from reduced aeolian dust input, which lowered the Ti content of the marls. Alternatively, increased Al input could also lower the ratio. When the Aegean input is high and dominates the terrigenous input, higher Al will lower the Ti/Al ratio so that it is no longer a suitable proxy for aeolian dust input. However, when the Aegean terrigenous contribution decreases, the Ti/Al ratio is influenced by the Ti associated with aeolian dust derived from North Africa and hence represents the aeolian fraction associated with marls.

[24] Si/Al undergoes no major variations throughout the Metochia section and the mean value of ~2.75 is slightly below the values reported for Pliocene sapropel-marl sediments [*Wehausen and Brumsack*, 2000] but is within the range of modern Saharan dust values [*Bergametti et al.*, 1989] (Figure 2). This indicates that there was a continuous input of North African material to the Metochia section during the late Miocene. Lower values than in the Pleistocene can be linked to higher Al input during the Miocene. Prior to ~8.5 Ma, Si/Al is slightly below the average, but it then generally increases. The Fe/Al ratio (Figure 3) is generally lower than the values reported for ODP Site 969 [*Wehausen and Brumsack*, 2000], but the values are still within the range of 0.35–0.7 reported for African dust by *Bergametti et al.* [1989] (Figure 2). The low Fe/Al ratios and the presence of four elevated values illustrate that Fe remobilization seems unlikely to have occurred in the majority of the marls. However, in isolated cases, Fe/Al peaks correspond with peaks in Mn/Al, indicating the possibility of remobilized Fe and Mn as the result of early diagenesis (Figure 3) [*van Santvoort et al.*, 1997]. When these intervals coincide with elevated Ni values (Figure 3), diagenetic processes are likely to dominate the signal in the marls, e.g., at ~9.0, ~7.9, and ~7.3 Ma. Diagenetic processes are known to dominate the magnetic and geochemical properties within intervals of eastern Mediterranean sediments [*Roberts et al.*, 1999; *Larrasoaña et al.*, 2003b]. While this appears to be the case in the Metochia section, such intervals are sporadic and are not representative of the entire sequence. These results are therefore taken to indicate that this is appropriate to interpret data from the Metochia section in terms of changes in terrigenous source areas.

[25] Apart from isolated diagenetically altered samples, Ni is unambiguously associated with ultramafic rocks, which are exclusive in the immediate region to the Aegean landmass. Ni/Al (Figure 3) undergoes important variations throughout the Metochia section, with higher values from the base of the record until ~8.4 Ma. These higher values are within a similar range as at ODP Site 969, which contains a mixture of sapropels and marls, with sapropels commonly being enriched in Ni [*Wehausen and Brumsack*, 2000]. Ni/Al values decrease after 8.4 Ma. Most of the Metochia samples are relatively unaffected by diagenetic alteration of the Ni/Al ratio; therefore the values imply a change in the source area of the material reaching the Metochia section.

[26] Here κ_{cfb} has low values at the base of the Metochia section, which increase steadily to ~8.5 Ma and then decreases (Figure 2). The low and fairly constant κ_{cfb} values suggest that the marls are dominated by the paramagnetic clay minerals and that magnetite is only a minor component. There is a minor gradual κ_{cfb} decrease in the upper part of the section, which might imply a drop in detrital

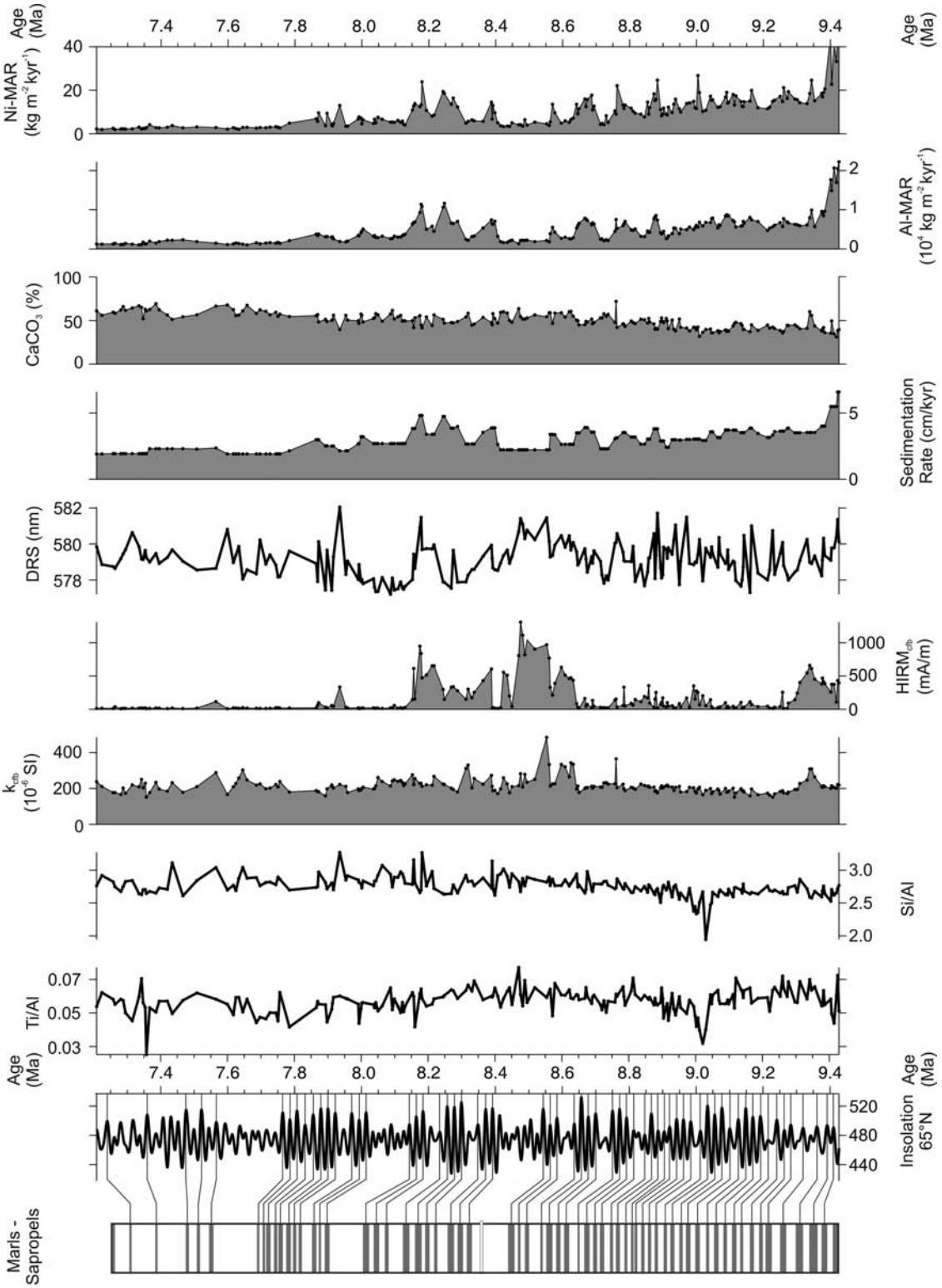

Figure 2. Profiles of geochemical, environmental magnetic, and diffuse reflectance spectrometry parameters with respect to age in the Metochia section. The elemental abundances are normalized to Al abundance or are shown in terms of mass accumulation rate. $HIRM_{cfb}$ is the ''hard'' isothermal remanent magnetization on a carbonate free basis. The stratigraphy of the Metochia section is shown in the far left, next to the insolation at 65°N [*Laskar et al.*, 2004]. Sapropels are indicated by gray bars and the homogenous marls, which are studied here, by the white intervals.

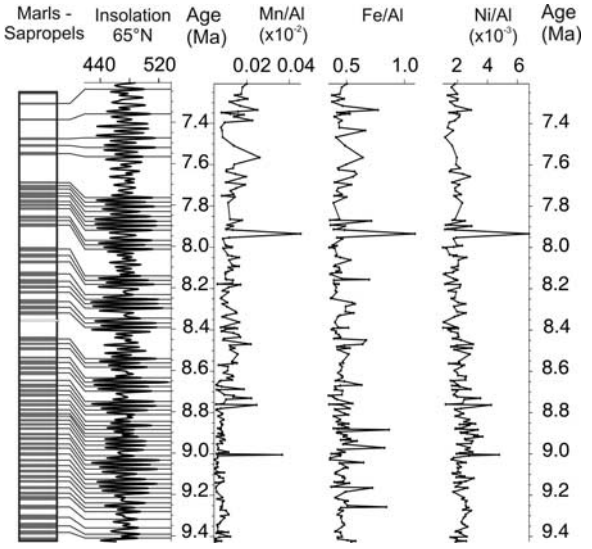

Figure 3. Profiles of elemental abundances normalized to Al abundance with respect to age in the Metochia section. Where high values of Mn/Al, Fe/Al, and Ni/Al correspond, e.g., at ~7.9 Ma, there is a hidden sapropel [cf. *Larrasoaña et al.*, 2006] (a sapropel layer has also been reported in this time interval in the Monte Gibliscemi section, Sicily [*Hilgen et al.*, 1995]). The stratigraphy of the Metochia section is shown to the left with gray intervals indicating sapropels, with white intervals indicating homogenous marls, next to the insolation at 65°N [*Laskar et al.*, 2004].

magnetite, along with an overall decrease in sedimentation in this time interval. However, κ_{cfb} does not follow the overall sedimentation rate trend, which steadily decreases throughout the section and then drops more sharply after 8.1 Ma (Figure 2).

[27] HIRM values indicate that the hematite/goethite content of the marls vary substantially (Figure 2). Prior to 8.1 Ma, $HIRM_{cfb}$ has the highest variability with periods of elevated hematite/goethite abundances in the marls. Also, the magnetite content probably varies slightly in this interval, as indicated by small changes in κ_{cfb}. Within two intervals (9.4–9.3 Ma and 8.65–8.15 Ma), $HIRM_{cfb}$ has maximum values (Figure 2); therefore the marls contain high amounts of hematite/goethite. These peaks correspond to the intervals described by *Krijgsman et al.* [1995] as containing a mixture of hematite and magnetite. Intermediate $HIRM_{cfb}$ values are present between 9.3 and 8.65 Ma. The marls should therefore still contain hematite/goethite in this time interval. After 8.15 Ma, $HIRM_{cfb}$ drops to its lowest values and remains low, indicating that hematite/goethite are only a minor component in the magnetic mineral fraction. *Krijgsman et al.* [1995] did not identify hematite in this time interval at Metochia.

[28] The dominant DRS wavelength fluctuates around 577–582 nm (Figure 2), which is within the lower range of the 580–595 nm envelope expected for hematite and goethite mixtures [*Madeira et al.*, 1997]. Prior to 8.7 Ma, values fluctuate around 580 nm and have highest values between 8.7 and 8.45 Ma. These peaks correspond with maximum $HIRM_{cfb}$ values and follow the observed pattern of hematite/goethite content. After 8.45 Ma, the values of the dominant wavelength become lower and fluctuate around ~579 nm, indicating the presence of at least traces of hematite and goethite in the marls, despite the low $HIRM_{cfb}$ (Figure 2).

4.2. Multivariate Statistics

[29] The selected input parameters for FCM and NLM (Table 1) represent the various environmental processes recorded within the Metochia sediments. Al is associated with terrigenous aluminosilicate minerals and can originate potentially from either the Aegean region or North Africa. Al-MAR is therefore used to indicate the total terrigenous supply to the Gavdos Basin. The marine component, $CaCO_3$, is expected to behave in an approximately inverse manner to Al-MAR.

Table 1. Input Parameters for the Cluster Analysis and What They Represent in the Fuzzy *c*-Means Cluster Analysis Solution

Input Parameter	"Simplified" Fuzzy *c*-Means Cluster Analysis Interpretation
Al-MAR (kg m^{-2} ka^{-1})	Total aluminosilicate input, overall terrestrial input
$CaCO_3$ (%)	Biogenic production, marine component
Mn/Al	Diagenetic changes in the marls
Ti/Al	Fluvial versus aeolian North African transport (when Aegean input is low)
Ni-MAR (kg m^{-2} ka^{-1})	Aegean input
$HIRM_{cfb}$ (mA/m)	Hematite and goethite, North African dust component

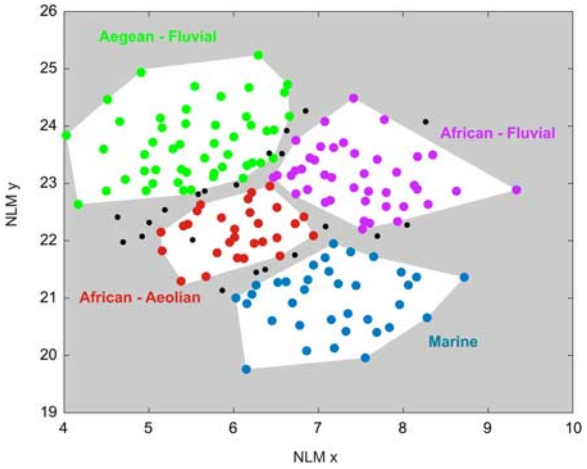

Figure 4. Nonlinear map of the four-cluster separation. Transitional cases are shown as small black dots. The axes on the nonlinear matching are arbitrary. The Aegean cluster is green, the humid North Africa cluster is purple, the arid North Africa cluster is red, and the marine productivity cluster is blue.

[30] $HIRM_{cfb}$ and Ti/Al are expected to typify the input of North African material. From the age profiles (Figure 2), $HIRM_{cfb}$ is expected to vary more than Ti/Al. Ti/Al responds to transport mechanisms from North Africa to eastern Mediterranean basins and can provide information on how the fluvial-aeolian system varied during the studied time interval. The relationship between the two North African input parameters is not straightforward in this case from examination of the univariate plots; FCM could provide insights into how the parameters are related.

[31] Al-MAR is used to represent the Aegean region. Unlike in the univariate analysis, the Ni-MAR is preferred over Ni/Al in the FCM and NLM analysis because the mass accumulation rate better describes the total input variation of Ni, which is a trace component in the sediment. In contrast, Ni/Al is used (Figure 3) to track diagenetic alteration and to provide a direct comparison with the results of *Wehausen and Brumsack* [2000] for an uplifted Crete during the Pliocene.

[32] Mn/Al is used to trace diagenetic processes in the marls because Mn is a redox sensitive element and is remobilized during diagenesis [*van Santvoort et al.*, 1997]. To balance the input parameters to avoid overrepresentation, some parameters are not used for FCM. These include the North African source area indicators Si/Al and Fe/Al, the dominant DRS wavelength, which represents hematite and goethite variations, and κ_{cfb}, which indicates terrigenous sediment input. The source areas or processes described by these parameters are either ambiguous or are already represented by the chosen input parameters, which are more sensitive to the specific processes of interest.

[33] While repeated runs of the algorithm, which were aimed at testing the stability of the solution, indicated that two-, three-, four-, and five-cluster solutions were viable from a statistical viewpoint, the four-cluster model seems to be the optimal cluster solution. The partitioning factor F' was maximized and the entropy H' was minimized [*Bezdek et al.*, 1984; *Vriend et al.*, 1988] in the two-cluster solution, but the four-cluster solution is a refined version of the lower cluster number solutions, as individual clusters split into coherent parts. The two-cluster solution separates the data into a "terrigenous" and "marine" cluster; the three-cluster solution further divides the "terrigenous" cluster into two separate groups, which is continued in the four-cluster solution. The five-cluster solution has small cluster sizes, which further divides the terrigenous clusters into smaller clusters and makes the solution uninterpretable. The four-cluster solution has 22 transitional versus 186 cluster-associated samples which is acceptable when studying the major and long-term changes rather than sample-to-sample variation. The locations of all the samples, including the transitional cases, are shown in the NLM plot (Figure 4). When the samples are grouped according to their FCM memberships, the NLM provides clear support for the four-cluster solution.

5. Discussion

5.1. Paleoenvironmental Interpretation

[34] Results of the FCM analysis enable highlighting of different paleoenvironmental settings that were present during the late Miocene. The positions of the cluster centers (Table 2) within the measurement space enable identification of the paleoenvironmental conditions represented. Description and interpretation of the clusters in terms of sediment input is provided in Figure 5, which indicates that two clusters are defined by changes in the terrigenous component (clusters 1 and 4) and that clusters 2 and 3 are characterized by changes in North Africa. The results demonstrate clearly that the cluster separation depends on changes in the overall terrigenous input, especially concerning the North African dust ($HIRM_{cfb}$) and Aegean-sourced sediment (Ni-MAR). As expected, the

Table 2. Locations of the Cluster Centers Within the Measurement Space for the Four-Cluster Model

	Cluster Center 1 Aegean Cluster	Cluster Center 2 Humid North African Cluster	Cluster Center 3 Arid North African Cluster	Cluster Center 4 Marine Productivity Cluster
Al-MAR (kg m^{-2} ka^{-1})	7343	4488	4160	1489
$CaCO_3$ (%)	40	49	51	60
Mn/Al	0.0065	0.0092	0.011	0.014
Ti/Al	0.0581	0.0554	0.0622	0.0552
Ni-MAR (kg m^{-2} ka^{-1})	15.84	8.65	9.92	2.84
$HIRM_{cfb}$ (mA/m)	97	31	341	15

marine component $CaCO_3$ increases as the terrigenous supply decreases.

[35] Examining Table 2 reveals that Mn/Al is consistently low across all the clusters, which demonstrates that diagenesis marginally influences the cluster solution. Samples associated with peaks in the Mn/Al profile (Figure 3) are transitional cases. Therefore environmental signals recorded by samples represented in the FCM can be considered to be of a primary origin. Cluster 1 is located in a measurement space with high terrigenous input and low $CaCO_3$ values. Al-MAR and Ni-MAR, in particular, have the highest values for any cluster center, which indicates the importance and predominance of terrigenous input, especially from the Aegean. Parameters that correspond to North African input ($HIRM_{cfb}$ and Ti/Al) have intermediate values. Ti/Al in this cluster is influenced by the high Al input from the Aegean, which should lower the ratio. Ti/Al therefore does not represent North African input pathways but rather reflects Aegean versus North African input for the Metochia section.

[36] The largest contrast to the terrigenous input represented by cluster center 1 is observed in cluster center 4, which is dominated by high $CaCO_3$ contents, suggesting that this cluster represents marine input. This hypothesis is supported by low values of the terrigenous indicator parameters, Al-MAR and Ni-MAR. The input parameters representing North African sources, $HIRM_{cfb}$ and Ti/Al, are also low in this cluster. On the basis of its position within the measurement space, it is apparent that cluster 4 represents predominantly marine input.

[37] Clusters 2 and 3 are distinguished on the basis of contrasts in North African source indicators. Terrigenous related parameters, especially concerned with the Aegean source and the marine component, have intermediate values in both clusters. Al input is no longer dominated by the Aegean source area but is a mixture from the Aegean and North Africa. Therefore, the cluster solutions can be interpreted as representing an African signal. Cluster center 2 has low $HIRM_{cfb}$ and Ti/Al values suggesting that the North African dust input is not important. Cluster center 3, on the other hand, is distinguished by high $HIRM_{cfb}$ values that indicated high aeolian dust supply. Ti/Al values are also highest in this cluster, which supports the importance of aeolian dust transport from North Africa.

[38] To summarize, cluster 1 ("Aegean cluster") has a high terrigenous component, with the most important source area being the Aegean landmass. It becomes gradually replaced by cluster 4 ("marine productivity cluster") via clusters 2 and 3. These clusters are influenced by changes in dust input from North Africa. Cluster 2 ("humid North African cluster") has low aeolian dust input, whereas cluster 3 ("arid North African cluster")

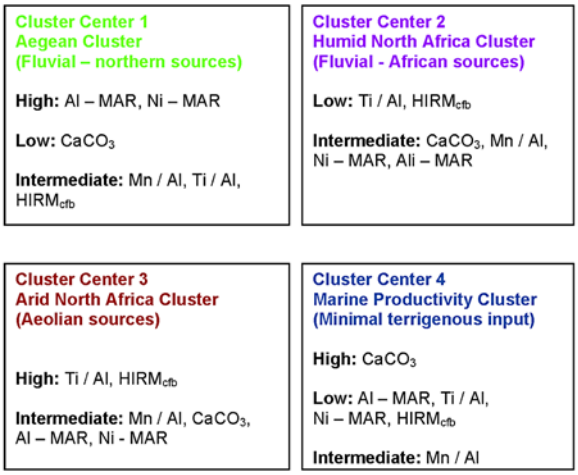

Figure 5. A schematic representation of the cluster center characteristics and their assigned source areas for the four cluster solution.

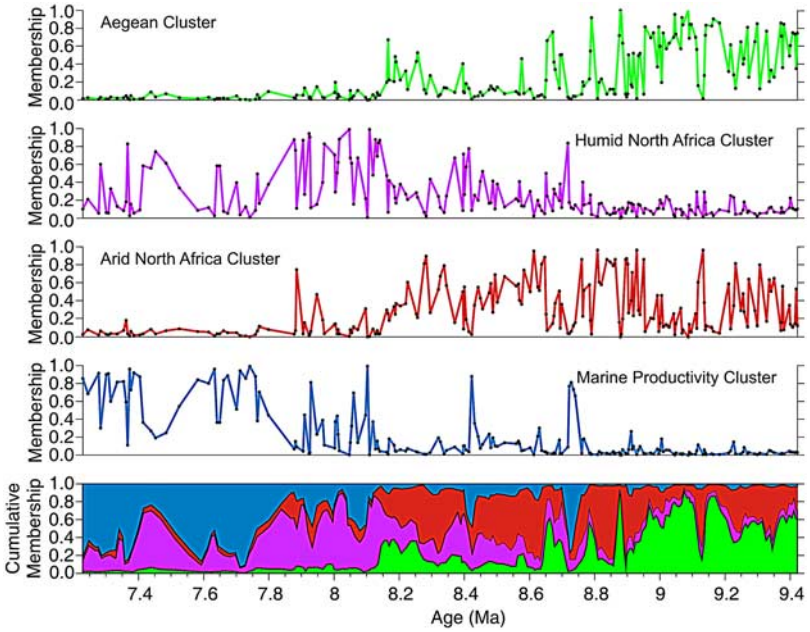

Figure 6. Fuzzy *c*-means cluster analysis membership variation of the different cluster centers of the Metochia section as a function of time. The membership values define the similarity of the sample to the clusters. The cumulative membership plot is smoothed using a three-point average. For cluster names and color coding, see Figure 4.

is characterized by high aeolian dust. Increased dust input described by cluster 3 suggests more arid paleoenvironmental conditions in North Africa, which allowed for enhanced dust production. Other relationships also appear, for example, Al-MAR, which is associated with terrigenous input, is highest in the Aegean cluster, which therefore indicates that a large amount of sediment comes directly from the Aegean landmass and dominates over the North African sources. This is not surprising considering the proximity of Gavdos to the former Aegean landmass, which was drained by a fluviolacustrine system toward the Gavdos Basin [*Fortuin*, 1978; *Meulenkamp et al.*, 1994; *van Hinsbergen and Meulenkamp*, 2006]. Al seems to be associated with an Aegean source; therefore it can explain the geochemical ratios that indicate a lower input from North African sources than during the Pliocene, as indicated by *Wehausen and Brumsack* [1998, 2000] (e.g., Fe/Al, Ti/Al). Especially in the Aegean cluster, low Ti/Al values can be explained by high Al abundance from Aegean sources, where this ratio reflects an Aegean versus North African signal. However, in the three other clusters, Al-MAR is intermediate or low, indicating a smaller Aegean contribution. Ti/Al variations in these clusters should therefore be related to changes in the African sediment transport system from more aeolian (arid North Africa) to more fluvial/less aeolian transport (humid North Africa).

[39] By considering the FCM membership values of the individual Metochia samples, it is possible to employ the FCM solution to reconstruct sedimentary inputs as a function of time (Figure 6). The dominant feature of the membership plot of the individual clusters indicates that the Aegean cluster is replaced over time by the marine productivity cluster via the North African clusters. On the basis that the depositional environment at Gavdos did not change during this time interval [*van Hinsbergen and Meulenkamp*, 2006], it is apparent that the changes observed in the cluster memberships represent modifications to the composition of the terrigenous component. The Aegean cluster is dominant prior to ~8.8 Ma and is replaced by the marine productivity cluster after ~8.1 Ma. Isolated peaks where the marine productivity cluster is dominant prior to ~8.1 Ma can be related to high $CaCO_3$ contents. Starvation of Aegean sediment supply after ~8.1 Ma can be linked to the late Miocene breakup of the Aegean landmass [*Meulenkamp et al.*, 1994; *van Hinsbergen and Meulenkamp*, 2006]. The breakup would have caused submergence of the landmass, resulting in drowning of the sediment source area. The arid North African cluster was dominant prior to ~8.15 Ma, when it "competed" with the Aegean cluster for dominance. The humid North African cluster became dominant after ~8.15 Ma, along with an increasing contribution from the marine productivity cluster. The marine

productivity cluster also has low Ti/Al values, therefore there appears to have been a change toward less aeolian input from North Africa, which is consistent with a previously proposed shift toward more humid conditions in North Africa during the late Miocene [e.g., *Ruddiman et al.*, 1989; *Griffin*, 1999].

6. Conclusions

[40] The sedimentation history of the Metochia section was investigated in detail using geochemical, environmental magnetic, and DRS parameters. The multiparameter data set was constructed in such a way that it was possible to discriminate between terrigenous material originating from North Africa and the Aegean region. Changes in sediment source area appear to have occurred between 8.4 and 8.2 Ma. These changes were not apparent by inspection of univariate data profiles alone. A multivariate approach using FCM and NLM was therefore employed to characterize a carefully chosen geochemical and magnetic data set to unravel relationships between different paleoenvironmental processes. A four-cluster solution was selected because it best describes the complicated interplay of late Miocene paleoenvironmental and tectonic changes. The cluster solution indicates a distinct decrease of terrigenous input from the Aegean region over time. This Aegean source is progressively replaced by an open marine signal dominated by primary productivity at ~8.1 Ma, with a minimal contribution from the Aegean region. This change can be linked to the late Miocene breakup of the Aegean landmass.

[41] Variations in North African dust input indicate that during the late Miocene both arid (aeolian) and humid (fluvial) phases were present. A switch toward less arid environmental conditions suggests less aeolian dust input after ~8.15 Ma, which indicates more humid conditions in North Africa.

Acknowledgments

[42] We are thankful for the laboratory assistance of T. Frederichs, L. Brück, C. Hilgenfeldt, and K. Enneking. Reviews by A.P. Roberts and an anonymous reviewer greatly improved the manuscript. This study was financed by the DFG International Graduate College EUROPROX.

References

Bergametti, G., L. Gomes, G. Coude-Gaussen, P. Rognon, and M.-N. Le Coustumer (1989), African dust observed over Canary Islands: Source-regions identification and transport pattern for some summer situations, *J. Geophys. Res.*, *94*, 14,855–14,864, doi:10.1029/JD094iD12p14855.

Bezdek, J. C. (1981), *Pattern Recognition With Fuzzy Objective Functions*, 256 pp., Plenum, New York.

Bezdek, J. C., R. Ehrlich, and W. Full (1984), The fuzzy c-means clustering algorithm, *Comput. Geosci.*, *10*, 191–203, doi:10.1016/0098-3004(84)90020-7.

Bloemendal, J., J. W. King, F. R. Hall, and S.-J. Doh (1992), Rock magnetism of Late Neogene and Pleistocene deep-sea sediments: Relationship to sediment source, diagenetic processes and sediment lithology, *J. Geophys. Res.*, *97*, 4361–4375, doi:10.1029/91JB03068.

Cande, S. C., and D. V. Kent (1995), Revised calibration of the geomagnetic polarity timescale for the Late Cretaceous and Cenozoic, *J. Geophys. Res.*, *100*, 6093–6095, doi:10.1029/94JB03098.

Chiapello, I., G. Bergametti, B. Chatenet, P. Bousquet, F. Dulac, and E. Santos Soares (1997), Origins of African dust transported over the northeastern tropical Atlantic, *J. Geophys. Res.*, *102*, 13,701–13,709, doi:10.1029/97JD00259.

Cornell, R. M., and U. Schwertmann (1996), The Iron Oxides: *Structure, Properties, Reactions, Occurrence, and Uses*, 573 pp., Weinheim, New York.

Deaton, B. C., and W. L. Balsam (1991), Visible spectroscopy—A rapid method for determining hematite and goethite concentration in geological materials, *J. Sediment. Petrol.*, *61*, 628–632.

Dekkers, M. J., C. G. Langereis, S. P. Vriend, P. J. M. van Santvoort, and G. J. de Lange (1994), Fuzzy c-means cluster analysis of early diagenetic effects on natural remanent magnetisation acquisition in a 1.1 Myr piston core from the central Mediterranean, *Phys. Earth Planet Inter.*, *85*, 155–171, doi:10.1016/0031-9201(94)90014-0.

deMenocal, P., J. Bloemendal, and J. W. King (1991), A rock-magnetic record of monsoonal dust deposition to the Arabian Sea: Evidence for a shift in the mode of deposition at 2.4 Ma, *Proc. Ocean Drill. Program Sci. Results*, *117*, 389–407.

Fortuin, A. R. (1978), Late Cenozoic history of eastern Crete and implications for the geology and geodynamics of the southern Aegean region, *Geol. Mijnbouw*, *57*, 451–464.

Foucault, A., and F. Mélières (2000), Palaeoclimatic cyclicity in central Mediterranean Pliocene sediments: The mineralogical signal, *Palaeogeogr. Palaeoclimatol. Palaeoecol.*, *158*, 311–323, doi:10.1016/S0031-0182(00)00056-0.

Griffin, D. L. (1999), The late Miocene climate of northeastern Africa: Uravelling the signals in the sedimentary succession, *J. Geol. Soc.*, *156*, 817–826, doi:10.1144/gsjgs.156.4.0817.

Hanesch, M., R. Scholger, and M. J. Dekkers (2001), The application of fuzzy c-means cluster analysis and non-linear mapping to a soil data set for the detection of polluted sites, *Phys. Chem. Earth, Part A*, *26*(11–12), 885–891, doi:10.1016/S1464-1895(01)00137-5.

Hilgen, F. J., W. Krijgsman, C. G. Langereis, L. J. Lourens, A. Santarelli, and W. J. Zachariasse (1995), Extending the astronomical (polarity) time scale into the Miocene, *Earth Planet. Sci. Lett.*, *136*, 495–510, doi:10.1016/0012-821X(95)00207-S.

Jacobshagen, V. (1986), *Geologie von Griechenland*, pp. 257–279, Borntraeger, Berlin.

King, J. W., and J. E. T. Channell (1991), Sedimentary magnetism, environmental magnetism, and magnetostratigraphy, *Rev. Geophys.*, *29*, 358–370.

Kouwenhoven, T. J., M.-S. Seidenkrantz, and G. J. van der Zwaan (1999), Deep-water changes: The near-synchronous disappearance of a group of benthic foraminifera from the Late Miocene Mediterranean, *Palaeogeogr. Palaeoclimatol.*

Palaeoecol., *152*, 259–281, doi:10.1016/S0031-0182(99)00065-6.

Kouwenhoven, T. J., F. J. Hilgen, and G. J. van der Zwaan (2003), Late Tortonian-early Messinian stepwise disruption of the Mediterranean Atlantic connections: Constraints from benthic foraminiferal and geochemical data, *Palaeogeogr. Palaeoclimatol. Palaeoecol.*, *198*, 303–319, doi:10.1016/S0031-0182(03)00472-3.

Krijgsman, W., F. J. Hilgen, C. G. Langereis, A. Santarelli, and W. J. Zachariasse (1995), Late Miocene magnetostratigraphy, biostratigraphy and cyclostratigraphy in the Mediterranean, *Earth Planet. Sci. Lett.*, *136*, 475–494, doi:10.1016/0012-821X(95)00206-R.

Kruiver, P. P., Y. S. Kok, M. J. Dekkers, C. G. Langereis, and C. Laj (1999), A pseudo-Thellier relative palaeointensity record, and rock magnetic and geochemical parameters in relation to climate during the last 276 kyr in the Azores region, *Geophys. J. Int.*, *136*, 757–770, doi:10.1046/j.1365-246x.1999.00777.x.

Kruiver, P. P., W. Krijgsman, C. G. Langereis, and M. J. Dekkers (2002), Cyclostratigraphy and rock-magnetic investigation of the NRM signal in late Miocene palustrine-alluvial deposits of the Librilla section (SE Spain), *J. Geophys. Res.*, *107*(B12), 2334, doi:10.1029/2001JB000945.

Larrasoaña, J. C., A. P. Roberts, E. J. Rohling, M. Winklhofer, and R. Wehausen (2003a), Three million years of monsoon variability over the northern Sahara, *Clim. Dyn.*, *21*, 689–698, doi:10.1007/s00382-003-0355-z.

Larrasoaña, J. C., A. P. Roberts, J. S. Stoner, C. Richter, and R. Wehausen (2003b), A new proxy for bottom-water ventilation in the eastern Mediterranean based on diagenetically controlled magnetic properties of sapropel-bearing sediments, *Palaeogeogr. Palaeoclimatol. Palaeoecol.*, *190*, 221–242, doi:10.1016/S0031-0182(02)00607-7.

Larrasoaña, J. C., A. P. Roberts, A. Hayes, R. Wehausen, and E. J. Rohling (2006), Detecting missing beats in the Mediterranean climate rhythm from magnetic identification of oxidized sapropels, *Phys. Earth Planet Inter.*, *156*, 283–293, doi:10.1016/j.pepi.2005.04.017.

Laskar, J. (1990), The chaotic motion of the solar system: A numerical estimate of the size of the chaotic zones, *Icarus*, *88*, 266–291, doi:10.1016/0019-1035(90)90084-M.

Laskar, J., P. Robutel, F. Joutel, M. Gastineau, A. C. M. Correia, and B. Levard (2004), A long-term numerical solution for the insolation quantities of the Earth, *Astron. Astrophys.*, *428*, 261–285, doi:10.1051/0004-6361:20041335.

Lourens, L. J., R. Wehausen, and H.-J. Brumsack (2001), Geological constraints on tidal dissipation and dynamical ellipticity of the Earth over the past three million years, *Nature*, *409*, 1029–1033, doi:10.1038/35059062.

Madeira, J., A. Bedidi, B. Cervelle, M. Pouget, and N. Flay (1997), Visible spectrometric indices of hematite (Hm) and goethite (Gt) content in lateritic soils: The application of a Thematic Mapper (TM) image for soil-mapping in Brasilia, Brazil, *Int. J. Remote Sens.*, *18*, 2835–2852, doi:10.1080/014311697217369.

Meulenkamp, J. E., and F. J. Hilgen (1986), Event stratigraphy, basin evolution and tectonics of the Hellenic and Calabro-Sicilian arcs, in *The Origin of Arcs*, edited by F.-C. Wezel, pp. 327–350, Elsevier, Amsterdam.

Meulenkamp, J. E., W. A. Van der Zwaan, and W. A. Van Wamel (1994), On Late Miocene to Recent vertical motions in the Cretan segment of the Hellenic arc, *Tectonophysics*, *234*, 53–72, doi:10.1016/0040-1951(94)90204-6.

Passier, H. F., M. J. Dekkers, and G. J. de Lange (1998), Sediment chemistry and magnetic properties in an anomalously reducing core from the eastern Mediterranean Sea, *Chem. Geol.*, *152*, 287–306, doi:10.1016/S0009-2541(98)00121-1.

Peterson, L. C., G. H. Haug, K. A. Hughen, and U. Röhl (2000), Rapid changes in the hydrological cycle of the Tropical Atlantic during the last glacial, *Science*, *290*, 1947–1951, doi:10.1126/science.290.5498.1947.

Postma, G., F. J. Hilgen, and W. J. Zachariasse (1993), Precession-punctuated growth of a late Miocene submarine-fan lobe on Gavdos (Greece), *Terra Nova*, *5*, 438–444, doi:10.1111/j.1365-3121.1993.tb00281.x.

Roberts, A. P., J. S. Stoner, and C. Richter (1999), Diagenetic magnetic enhancement of sapropels from the eastern Mediterranean Sea, *Mar. Geol.*, *153*, 103–116, doi:10.1016/S0025-3227(98)00087-5.

Ruddiman, W. F., et al. (1989), Late Miocene to Pleistocene evolution of climate in Africa and the low-latitude Atlantic: Overview of Leg 108 results, *Proc. Ocean Drill. Program Sci. Results*, *108*, 463–484.

Sammon, J. W. (1969), A non-linear mapping for data structure analysis, *IEEE Trans. Comput.*, *C18*, 401–409, doi:10.1109/T-C.1969.222678.

Schenau, S. J., A. Antonarakou, F. J. Hilgen, L. J. Lourens, I. A. Nijenhuis, C. H. van der Weijden, and W. J. Zachariasse (1999), Organic-rich layers in the Metochia section (Gavdos, Greece): Evidence for a single mechanism of sapropel formation during the past 10 My, *Mar. Geol.*, *153*, 117–135, doi:10.1016/S0025-3227(98)00086-3.

Schmidt, A. M., T. von Dobeneck, and U. Bleil (1999), Magnetic characterization of Holocene sedimentation in the South Atlantic, *Paleoceanography*, *14*, 465–481, doi:10.1029/1999PA900020.

Stoner, J. S., J. E. T. Channell, and C. Hillaire-Marcel (1996), The magnetic signature of rapidly deposited detrital layers from the deep Labrador Sea: Relationship to North Atlantic Heinrich layers, *Paleoceanography*, *11*, 309–325, doi:10.1029/96PA00583.

Urbat, M., M. J. Dekkers, and K. Krumsiek (2000), Discharge of hydrothermal fluids through sediment at the Escanda Trough, Gorda Ridge (ODP Leg 169), Assessing the effects on the rock magnetic signal, *Earth Planet. Sci. Lett.*, *176*, 481–494, doi:10.1016/S0012-821X(00)00024-8.

van Hinsbergen, D. J., and J. E. Meulenkamp (2006), Neogene supradetachment basin development on Crete (Greece) during exhumation of the South Aegean core complex, *Basin Res.*, *18*, 103–124, doi:10.1111/j.1365-2117.2005.00282.x.

van Santvoort, P. J. M., G. J. de Lange, C. G. Langereis, and M. J. Dekkers (1997), Geochemical and paleomagnetic evidence for the occurrence of "missing" sapropels in eastern Mediterranean sediments, *Paleoceanography*, *12*, 773–786, doi:10.1029/97PA01351.

Venkatarathnam, K., and W. B. F. Ryan (1971), Dispersal patterns of clay minerals in the sediments of the eastern Mediterranean Sea, *Mar. Geol.*, *11*, 261–282, doi:10.1016/0025-3227(71)90028-4.

Vlag, P. A., P. P. Kruiver, and M. J. Dekkers (2004), Evaluating climate change by multivariate statistical techniques on magnetic and chemical properties of marine sediments (Azores region), *Palaeogeogr. Palaeoclimatol. Palaeoecol.*, *212*, 23–44.

Vriend, S. P., P. F. M. van Gaans, J. J. Middelburg, and A. de Nijs (1988), The application of fuzzy c-means cluster analysis and non-linear mapping to geochemical data sets: Examples from Portugal, *Appl. Geochem.*, *3*, 213–224, doi:10.1016/0883-2927(88)90009-1.

Wedepohl, K. H. (1969), Composition and abundances of common igneous rocks, in *Handbook of Geochemistry*, edited by K. H. Wedepohl, 444 pp., Springer, Berlin.

Wehausen, R., and H.-J. Brumsack (1998), The formation of Pliocene Mediterranean sapropels: Constraints from high-resolution major and minor element studies, *Proc. Ocean Drill. Program Sci. Results*, *160*, 207–217.

Wehausen, R., and H.-J. Brumsack (2000), Chemical cycles in Pliocene sapropel-bearing and sapropel barren eastern Mediterranean sediments, *Palaeogeogr. Palaeoclimatol. Palaeoecol.*, *158*, 325–352, doi:10.1016/S0031-0182(00)00057-2.